

Received July 22, 2019, accepted August 4, 2019, date of publication August 7, 2019, date of current version August 21, 2019.

Digital Object Identifier 10.1109/ACCESS.2019.2933753

# Construction of Quasi-Cyclic Low Density Parity Check Codes for Magnetic Induction Communication

HUA XU<sup>1</sup>, (Member, IEEE), YANJING SUN<sup>2</sup>, (Member, IEEE),  
AND WENJUAN SHI<sup>1</sup>, (Member, IEEE)

<sup>1</sup>School of Physics and Electronic Engineering, Yancheng Teachers University, Yancheng 224007, China

<sup>2</sup>School of Information and Control Engineering, China University of Mining and Technology, Xuzhou 221116, China

Corresponding author: Hua Xu (xuhua@yctu.edu.cn)

This work was supported by the National Natural Science Foundation of China under Grant 61771417.

**ABSTRACT** The magnetic induction (MI) communication has been proved to be an effective method in the wireless underground sensor networks (WUSN). MI communication system based on quasi-cyclic low density parity check (QC-LDPC) codes is expected to improve the transmission performance in WUSN for its good performance and hardware friendliness. In this paper, we aim to construct an optimized QC-LDPC code with low encoding complexity for MI communication system. Firstly, we present a novel method, magnetic induction - protograph extrinsic information transfer (MI-PEXIT) algorithm, which can evaluate the performance of the QC-LDPC codes and predict the distance threshold for successfully transmission of the direct MI communication. Then, we combine the discrete particle swarm optimization (PSO) algorithm with the MI-PEXIT algorithm, and propose a novel scheme DPMIP method to optimize the QC-LDPC codes for MI communication system. Furthermore, two groups of QC-LDPC codes with low encoding complexity are constructed by the proposed DPMIP algorithm, which have different code parameters and different coil parameters. Simulation results validate the superiority of the proposed QC-LDPC codes for MI communication in WUSN, and the proposed codes also can achieve a good trade-off between the complexity and the performance.

**INDEX TERMS** Magnetic induction communication, mutual information, distance threshold, QC-LDPC codes, EXIT chart.

## I. INTRODUCTION

Wireless underground sensor networks (WUSN) have aroused much interest in recent years. It can be used in pipeline monitoring, mine rescue, intelligent agriculture and other underground applications. The traditional electromagnetic (EM) wave communication suffers from high attenuation in WUSN because its propagation medium is no longer air but rock, soil and water. Magnetic induction (MI) communication is a promising technique to deal with the underground challenge, which can achieve a better performance than the EM wave communication [1], [2].

There are two main methods for MI communication, direct MI and MI waveguides. The direct MI utilizes a couple of coils as the transmitter and the receiver. The MI waveguides

use some relay points, which are only single coils without any processing device, besides the transmitter coil and the receiver coil [1], [3]–[11].

MI-based signal transmission has already been employed to transfer the information and power simultaneously [12]. In [6], the error propagation of MI communication system attenuates its signal transmission performance, and channel coding is necessary to improve the performance of signal transmission for MI communication in WUSN. Thus, we can adopt a strong channel coding scheme in MI communication system to mitigate the effect of the error propagation. However, little work is done on the channel code optimization of MI communication so far as we know.

Low-density parity-check (LDPC) codes have been studied in many channels such as binary erasure channel (BEC), additive white Gaussian noise (AWGN) channel, Rayleigh channel and relay channel [13]–[18]. They have already been

The associate editor coordinating the review of this manuscript and approving it for publication was Ning Zhang.

adopted in WUSN [19]. The relation between the underground soil moisture and the performance of communication is investigated. Experiment results show that using LDPC codes in WUSN can effectively improve its performance. However, only the traditional EM wave communication in WUSN is considered in [19]. MI communication based on LDPC codes in WUSN is expected to obtain a better performance than that of EM wave communication.

As an important subclass of LDPC codes, the QC-LDPC code can achieve a good trade-off between performance and complexity for its simple structure and hardware friendliness [20]–[22]. It has already been used in several advanced communication standards like 802.16e and 802.11n [23]–[25]. For WUSN, small size and low power consumption are necessary for the sensor nodes. Therefore, the QC-LDPC code is a good choice for MI communication in WUSN.

To reduce the energy consumption of the encoder for MI communication in WUSN, QC-LDPC codes with low encoding complexity are expected to be a better way which can be encoded directly from the parity check matrix in a simple recursive manner [26].

MI channel model is given in [1]. However, the channel coding is not considered in [1]. In this paper, we aim to propose a method to design QC-LDPC codes with low encoding complexity for MI communication system in WUSN.

The main contributions of this paper are as follows.

(1) We propose a new method, MI-PEXIT algorithm, to evaluate the coil distances of the MI communication system based on QC-LDPC codes. It can provide an easy way to predict the coil distance for successfully transmission of a given QC-LDPC codes for the MI communication system. Meanwhile, we infer that there is a “distance threshold effect” for the QC-LDPC codes of MI communication system by using the MI-PEXIT algorithm, which can predict the coils distance for successfully transmission.

(2) We combine the discrete PSO algorithm with the MI-PEXIT algorithm, and then propose a novel scheme, DPMIP algorithm, to optimize the QC-LDPC codes for MI communication system. The parity check matrices of the optimized QC-LDPC codes can be constructed, and meanwhile their corresponding distance thresholds also can be obtained by the proposed DPMIP algorithm.

In this study, the distance threshold evolution and the mutual information evolution during the optimization for different QC-LDPC codes are given. Furthermore, the bit error rate (BER) performance are compared among the optimized QC-LDPC codes besides the comparison between the proposed codes and the 802.16e code. Note that the 802.16e code is the QC-LDPC code used in the 802.16e standards, and it is designed for the traditional EM wave communication.

This paper is organized as follows. The related work are reviewed in Sect.2, and the preliminaries of MI channel model and QC-LDPC codes are given in Sect.3. In Sect.4, we firstly give the MI communication model based on QC-LDPC codes. Then, the proposed MI-PEXIT algorithm

and DPMIP algorithm are described. In Sect.5, two groups of QC-LDPC codes are constructed by the proposed DPMIP algorithm. In the simulation, we compare the pathloss of different coil parameters. Then, we give the base matrices and the  $\mathbf{H}$  matrices of the proposed QC-LDPC codes. Furthermore, we describe the mutual information evolution of the proposed QC-LDPC codes, and compare their BER performance. Finally, the conclusion of this paper is given in Sect.6.

## II. RELATED WORK

The path loss of the direct MI and the MI waveguide were analysed in detail in [1], which is an important contribution to the MI communication. The channel capacity, the network capacity and the reliability of MI-based WUSN were investigated, and the closed form of the channel capacity of the MI channel was given in [4]. Furthermore, to increase the network throughput of the MI waveguide, a tree-based WUSN was investigated, in which the sensor nodes transmitted the signal by MI communication [5], [27].

Besides the theoretical analysis, a testbed of several MI communication systems was developed, including the direct MI and the MI waveguide. This study provides a guidelines for implementing a MI communication testbed [7]. Different underground materials may lead to different attenuation properties. Thus, for MI communication, the attenuation properties were studied in detail when the signal passed through the most common rocks and the minerals [2]. This work provides an important advice for designing the MI communication system and location system.

To achieve optimal energy savings and throughput gain, a distributed cross-layer protocol is proposed for MI-based WUSN. Simulation results show that the proposed scheme can effectively improve the energy savings and the throughput efficiency [28]. For the traditional EM wave communication in WUSN, the performance of the signal transmission highly depends on the medium of the underground environment [19].

The performance of the signal transmission in WUSN is increased when the rate compatible LDPC codes are adopted in the system. However, these LDPC codes are constructed randomly which are not suitable for hardware implementation, and they are not good choice for MI-based WUSN for their high energy consumption [19]. Meanwhile, EM wave communication in WUSN suffers more attenuation than MI communication. Therefore, MI communication system using QC-LDPC codes deserves to be studied to improve the performance of MI-based WUSN.

Density evolution (DE) and Gaussian approximation (GA) are two methods to evaluate the performance of LDPC codes. They are usually used to be combined with the optimization method to search the optimal LDPC codes for a certain channel [15], [29]. Extrinsic information transfer (EXIT) chart method has been widely used in performance evaluation and design of LDPC codes for its accuracy and simplicity.

To accurately evaluate the threshold of the protograph LDPC codes, a protograph EXIT (PEXIT) method is

proposed in [30], and it has also been used to find the threshold of QC-LDPC codes [17], [31], [32]. Therefore, it is expected to be used to evaluate the QC-LDPC codes of the MI communication system.

In this study, we develop the MI-PEXIT algorithm to track the mutual information evolution for a certain QC-LDPC code of MI communication system, which can predict the transmission distance between the two coils. Then, we combine this method with the discrete (binary) PSO algorithm, and propose the DPMIP algorithm, to search the optimal QC-LDPC codes with predetermined code parameters and coil parameters.

### III. PRELIMINARIES

In this section, we briefly review some concepts of MI channel model and QC-LDPC codes.

#### A. MI CHANNEL MODEL

In terms of MI communication, the information is conveyed by using the coils of wire. The channel model of MI communication is described as Fig.1 and Fig.2. MI transmitter coil and receiver coil are given in Fig.1, where  $a_t$  and  $a_r$  are the radii of the transmitter coil and receiver coil, respectively, and  $d$  is the distance between the two coils.

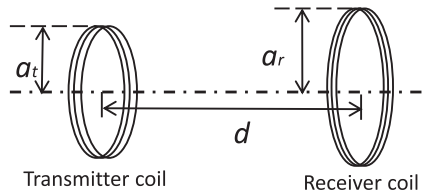


FIGURE 1. MI coils of transmitter and receiver.

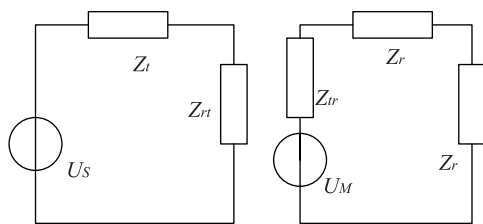


FIGURE 2. Equivalent circuit.

Note that the signal in the transmitter coil induce the corresponding signal in the receiver coil, and thus the two coils can be modelled as the primary coil and the secondary coil of a transformer. To further simplify the analyse, the equivalent circuit is given in Fig.2.

$U_S$  is the battery of the transmitter coil, and  $U_M$  is the induced voltage on the receiver coil;  $Z_t$  and  $Z_r$  are the self impedances of the transmitter coil and the receiver coil, respectively;  $Z_L$  is the load impedance.  $Z_{rt}$  is the influence of the receiver on the transmitter, and  $Z_{tr}$  is the influence of the transmitter on the receiver. The received power and the

transmission power can be described as follows [1].

$$P_r(d) = Re \left\{ \frac{Z_L \times U_M^2}{(Z_{tr} + Z_r + Z_L)^2} \right\} \quad (1)$$

$$P_t(d) = Re \left\{ \frac{U_S^2}{Z_t + Z_{rt}} \right\} \quad (2)$$

The details of the MI channel model can refer to [1].

Low energy consumption of the node is necessary for WUSN. MI signal transmission depends on the coupling of the wire coils in the near field, and it has lower energy consumption than EM waves transmission [28].

The transmission power of MI system is composed of the induced power and the coil power, which is consumed at the receiver and the coil resistance, respectively. Note that both of the transmission power and the receiving power highly depends on the transmission distance between the coils. For MI communication, there is nearly no power wasted on radiation if the distance is small enough, and thus almost all the power of the transmission coil can be conveyed to the receiving coil.

However, if the distance increases, the receiving power will be less. Note that the power is not really lost, and it is just not transmitted to the receiver. The path loss of the MI communication system is described as (3) [1].

$$L_{MI}(d) = 6.02 + 60lgd + 10lg \frac{N_t}{N_r a_t^3 a_r^3} \quad (3)$$

where  $d$  is the transmission distance;  $N_t$  and  $N_r$  are the number of turns of the transmitter coil and receiving coil;  $a_t$  and  $a_r$  are the radii of the transmission coil and the receiving coil.

#### B. QC-LDPC CODES

In this section, some definitions of QC-LDPC codes are given firstly. Then, QC-LDPC codes with low encoding complexity is described [26].

The parity check matrix of a QC-LDPC code,  $\mathbf{H}$ , is a binary matrix, which is composed of smaller square blocks. These blocks are the sub-matrices of  $\mathbf{H}$ , which are circulant permutation matrices or zero matrices. It may be described as follows.

$$H = \begin{bmatrix} P^{t_{00}} & \dots & P^{t_{0(N-2)}} & P^{t_{0(N-1)}} \\ P^{t_{10}} & \dots & P^{t_{1(N-2)}} & P^{t_{1(N-1)}} \\ \dots & \dots & \dots & \dots \\ P^{t_{(M-1)0}} & \dots & P^{t_{(M-1)(N-2)}} & P^{t_{(M-1)(N-1)}} \end{bmatrix} \quad (4)$$

where  $P^{t_{ij}}$  is a circulant permutation matrix or zero matrix with  $L \times L$ ,  $t_{ij} \in \{0, 1, 2, \dots, L - 1, \infty\}$ . The size of  $\mathbf{H}$  is  $ML \times NL$ . Note that if  $P^{t_{ij}}$  is a circulant permutation matrix, it can be constructed by cyclically shifting the row of the identity matrix by  $t_{ij}$  times. The matrix  $P$  is usually

defined as follows.

$$P = \begin{bmatrix} 0 & 1 & 0 & \cdots & 0 \\ 0 & 0 & 1 & \cdots & 0 \\ \vdots & \vdots & \vdots & \ddots & \vdots \\ 0 & 0 & 0 & \cdots & 1 \\ 1 & 0 & 0 & \cdots & 0 \end{bmatrix}_{L \times L} \quad (5)$$

However, if  $P^{t_{ij}}$  is a zero matrix, it is denoted as  $P^\infty$  or  $P^{-1}$  [16], [33].

The threshold of a QC-LDPC code is important to its performance evaluation. To evaluate the threshold, the binary base matrix of the QC-LDPC code,  $B(H)$ , has to be given besides the exponent matrix of a QC-LDPC code [32]. For example, the binary base matrix of  $\mathbf{H}$  is defined as (6).

$$B_1(H) = \begin{bmatrix} 0 & 1 & 1 \\ 1 & 0 & 1 \\ 0 & 0 & 1 \end{bmatrix} \quad (6)$$

where “0” refers to the zero sub-matrix in  $\mathbf{H}$ , “1” refers to the circulant permutation matrix in  $\mathbf{H}$ . Based on the binary base matrix, the corresponding exponent matrix is described as (7).

$$E_1(H) = \begin{bmatrix} -1 & t_{01} & t_{02} \\ t_{10} & -1 & t_{12} \\ -1 & -1 & t_{22} \end{bmatrix} \quad (7)$$

where “-1” corresponds to the zero submatrix and other entries correspond to the circulant permutation matrix in  $\mathbf{H}$  [26]. The position of “0” is determined when the base matrix of the QC-LDPC code is constructed. Then, the position of “-1” is determined in the exponent matrix.

Therefore, construction of the  $\mathbf{H}$  matrix of QC-LDPC codes can be reduced to the problem of constructing the binary base matrix  $\mathbf{B}(\mathbf{H})$  and the exponent matrix  $\mathbf{E}(\mathbf{H})$ , which have smaller size than  $\mathbf{H}$ .

To realize a low-complexity encoder, the matrix  $\mathbf{H}$  of a QC-LDPC code is usually divided into an information part and a parity part. A semi-deterministic approximate lower triangular (ALT) form of the parity part for the parity check matrix is proposed, and it achieves a better performance and more flexible design of QC-LDPC codes [26].

The  $\mathbf{H}$  matrix with low encoding complexity considered in this study, is described by the following equation:

$$H_{ML \times NL} = [(H_I)_{ML \times KL} | (H_P)_{ML \times ML}], \quad (8)$$

where  $H_I$  is the information portion and  $H_P$  is the parity portion of the  $\mathbf{H}$  matrix [26].  $NL$  is the code length of the QC-LDPC code,  $ML$  is the length of the parity bits, and  $KL$  is the length of the information bits, where  $NL = KL + ML$ .

Furthermore, to facilitate the encoding of QC-LDPC codes, the parity portion of the  $\mathbf{H}$  matrix has to be constructed in the

following form [26].

$$H_P = \begin{bmatrix} 0 & I & 0 & \cdots & 0 & 0 \\ 0 & h_{1,K+1} & I & \cdots & 0 & 0 \\ 0 & h_{2,K+1} & h_{2,K+2} & \cdots & 0 & 0 \\ \vdots & \vdots & \vdots & \ddots & \vdots & \vdots \\ P^{a_{ij}} & h_{M-3,K+1} & h_{M-3,K+2} & \cdots & I & 0 \\ I & h_{M-2,K+1} & h_{M-2,K+2} & \cdots & I & I \\ P^{a_{ij}} & h_{M-1,K+1} & h_{M-1,K+2} & \cdots & 0 & I \end{bmatrix} \quad (9)$$

where  $h_{ij}$  is the submatrix of the parity check matrix  $\mathbf{H}$ . It should be noted that all of the column weights of  $H_P$  are two, with the exception of the first column, which are the same as those of the dual-diagonal structure in 802.16e [23].

For the QC-LDPC codes with  $H_P$  as equation (9), the encoding problem is reduced to generate parity bits based on the information bits and  $\mathbf{H}$  matrix in a very simple recursive manner. The information bits are divided into  $K$  sub-blocks,  $d_0, d_1, d_2, \dots, d_{K-1}$ . Then, we obtain  $M$  sub-blocks,  $p_0, p_1, p_2, \dots, p_{M-1}$ .

The details of the encoding procedure of QC-LDPC codes with low encoding complexity may refer to [26].

#### IV. PROPOSED CONSTRUCTION SCHEME: DPMIP ALGORITHM

In this section, we propose a novel scheme to construct the QC-LDPC codes for MI channel, DPMIP algorithm, which combines the discrete PSO algorithm with the MI-PEXIT method. Firstly, we give the block diagram of the MI communication system based on QC-LDPC codes. Then, we describe the procedure of the proposed DPMIP algorithm.

##### A. MI COMMUNICATION SYSTEM BASED ON QC-LDPC CODES

The block diagram of the MI communication system based on QC-LDPC codes is given as Fig.3.

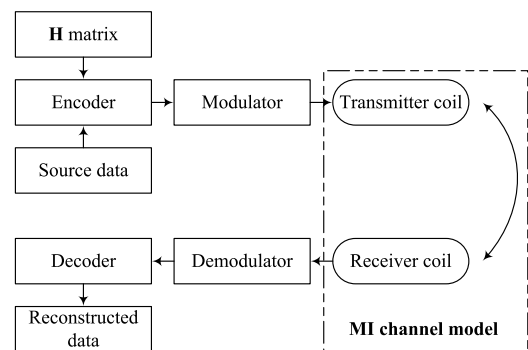


FIGURE 3. MI communication system based on QC-LDPC codes.

In Fig.3, the source data is encoded via the  $\mathbf{H}$  matrix of the QC-LDPC code. Note that we construct the QC-LDPC codes with low encoding complexity in this study, and encoding can be implemented in a simple recursive manner directly by  $\mathbf{H}$ . Then the encoded data sequences are modulated, and

they are transmitted through the MI channel. Furthermore, the receiver coil are induced by the transmitted signal, and then they are demodulated and decoded. Finally, the reconstructed data can be obtained and the signal transmission over the MI channel is accomplished.

Note that for MI communication in underground environment, it has less channel variations than that of the EM waves communication. The thermal vibration of circuit elements is the main noise source [28].

### B. PSO ALGORITHM

The PSO algorithm was proposed in [34], which is an effective method to deal with the non-linear, multiobjective optimization problem. It has already been adopted in a lot of fields like antenna design, data fusion, filter design [35]–[39].

The key point of the PSO algorithm is the “particle evaluation”. Consider there are many particles in the solution space, and each particle corresponds to one solution. We can use a fitness function to evaluate each particle. Then we will have two “best” values during each iteration. One is the particle best (*pbest*), which is the best fitness value of each individual particle so far. The other is the global best (*gbest*), which is the best fitness value among all the *pbest*. Note that the particles update their positions with a given velocity toward the final best solution during each iteration.

There are two types of the PSO algorithm, continuous PSO and discrete PSO, which are real-number and binary for the solution space, respectively [35].

The procedure of the PSO algorithm is given as follows.

1. Initialization. Each particle is initialized randomly.
2. Evaluation. The fitness value of each particle is obtained via the fitness function. For each particle, if the fitness value is better than *pbest* in the history, set the current fitness value be the new *pbest*. Then, we let the best one be *gbest*, which is compared among all the particles.
3. Update. The velocity of the particle is updated as follows.

$$V^i = wV^{i-1} + c_1\eta_1(P^{i-1} - X^{i-1}) + c_2\eta_2(G^{i-1} - X^{i-1}) \quad (10)$$

The position of the particle is updated as follows.

$$X^i = X^{i-1} + V^i, \quad (11)$$

where  $V^i$  is the velocity to be updated, and  $i$  is the number of iterations,  $P^{i-1}$  and  $G^{i-1}$  are the *pbest* and *gbest* values after  $i - 1$  iterations, respectively, and  $X^{i-1}$  is the position of the particle after  $i - 1$  iterations.

4. Stop Criterion. If the predetermined maximum number of iterations is achieved, the iteration stops.

Note that in this study, the variables to be optimized are the parity check matrix of QC-LDPC codes. Thus, we have to use the discrete (binary) PSO algorithm.

### C. MI-PEXIT ALGORITHM

To evaluate each particle in PSO algorithm, it is very important to evaluate the fitness value effectively and accurately. In this section, we propose a novel method, MI-PEXIT algorithm, to evaluate the QC-LDPC codes for MI communication system, which can track the mutual information evolution during the iteration.

There is an important property for LDPC codes in the EM wave communication which is called “noise threshold effect” [15]. Therefore, we infer that there is “distance threshold effect” for MI communication based on QC-LDPC codes.

Consider a MI communication system based on LDPC codes, if the transmission distance  $d < d^*$ , which is the distance threshold, and then the bit error rate converges to zero with infinity code lengths; if the distance  $d > d^*$ , and then the error probability is always bounded away from zero. The distance threshold is an important parameter which can predict the performance of the MI communication system based on QC-LDPC codes. The simulation results in this study demonstrate the “distance threshold effect”.

In this study, we use the MI-PEXIT algorithm to find the distance threshold of the QC-LDPC codes, which is the fitness value for the PSO algorithm.

For LDPC codes, the Tanner graph is usually used to describe the message propagation among the variable nodes and check nodes [15], [20], [29]. To better describe the presented algorithm, a Tanner graph model of the QC-LDPC code is given as Fig.4.

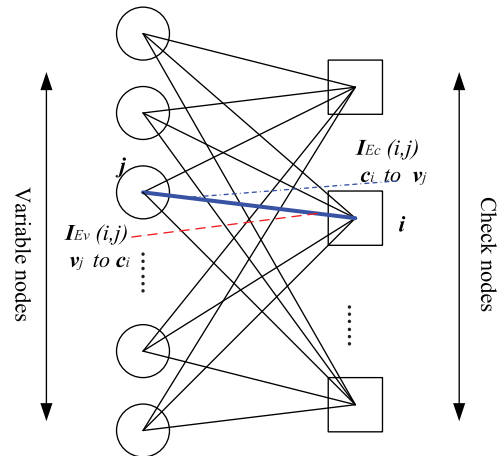


FIGURE 4. Tanner graph of the QC-LDPC code.

In Fig.4, the variable nodes in the left correspond to the columns of the  $\mathbf{H}$  matrix, and the check nodes in the right correspond to its row. The edges between the variable nodes and the check nodes correspond to “1” in the  $\mathbf{H}$  matrix. Then, we give the following definitions.

$I_{ch}$ : the mutual information between the channel observation and the associated codeword bit.



$I_{Ev}(i, j)$ : the mutual information between the message from  $v_j$  node to  $c_i$  node and the associated codeword bit. Note that the message is propagated on the edges  $e_{i,j}$  between  $v_j$  and  $c_i$ .

$I_{Ec}(i, j)$ : the mutual information between the message from  $c_i$  node to  $v_j$  node and the associated codeword bit.

$I_{Av}(i, j)$ : the a priori mutual information between one input message and the codeword bit associated to the variable node.

$I_{Ac}(i, j)$ : the a priori mutual information between one input message and the associated codeword bit.

$I_{APP}(j)$ : the mutual information between the a posteriori probability log-likelihood ratio  $LLR^{(j)}$  and the associated codeword bit  $x_j$ .

Note that the a posteriori probability log-likelihood ratio  $LLR^{(j)}$  is given as (12).

$$LLR^{(j)} = \ln \frac{Pr(x_j = +1|r)}{Pr(x_j = -1|r)} \quad (12)$$

where  $r$  is the received signal vector over the channel. Other details of the above definitions and the message propagation model may refer to [30].

The MI-PEXIT algorithm is described as follows. We assume that there are  $N$  variable nodes and  $M$  check nodes, which corresponds to  $H$  matrix with size  $M \times N$ . The edge between the  $j$ -th node and the  $i$ -th node is set as  $e_{i,j}$ .

1.Initialization.

- (1) Distance initialization. Let the coil distance be an initialized value  $d$ .
- (2) Mutual information  $I_{Av}(i, j)$  initialization. Let the mutual information  $I_{Av}(i, j)$  be zero,  $\forall i=0, 1 \dots M-1, j=0, 1 \dots N-1$ .

2.Update.

- (1) Mutual information  $I_{ch}$ . we denote  $J(\sigma)$  as the capacity of the channel, which is given as follows [40].

$$J(\sigma) = 1 - \int_{-\infty}^{\infty} \frac{1}{\sqrt{2\pi}\sigma^2} e^{-\frac{(y-\sigma^2/2)^2}{2\sigma^2}} \log_2(1+e^{-y}) dy \quad (13)$$

Furthermore, we have the mutual information as follows.

$$I_{ch}^{(j)} = J(\sigma_{ch,j}), \quad \forall j = 0, 1 \dots N-1 \quad (14)$$

Note that the variance of the channel input to the  $j$ -th variable node,  $\sigma_{ch,j}^2$ , is given in (15).

$$\sigma_{ch,j}^2 = 8R \times f(d_{V_j}) \quad (15)$$

where  $d_{V_j} = d$  is the transmission distance between the coils, and  $R$  is the code rate of the QC-LDPC codes.  $f(d_{V_j})$  can be calculated as follows [1].

$$f(d_{V_j}) = P_t - L_{MI} - P_n \quad (16)$$

where  $P_t$ ,  $L_{MI}$  and  $P_n$  are the transmission power, the path loss and the noise power, respectively. Note that  $L_{MI}$  is given in (3), which is the function of the transmission distance between the coils.

- (2) Mutual information  $I_{Ev}(i, j)$ . This is the mutual information associated with the message from the variable node to check node. We have the following equation.

$$I_{Ev}(i, j) = J(\sqrt{\sigma_{Ev}}) \quad (17)$$

where  $j = 0, 1 \dots, N-1$  and  $i = 0, 1 \dots, M-1$ .

- (3) Mutual information update for check nodes.

$$I_{Ac}(i, j) = I_{Ev}(i, j). \quad (18)$$

- (4) Mutual information update from check nodes to variable nodes.

$$I_{Ec}(i, j) = 1 - J(\sqrt{\sigma_{Ec}}) \quad (19)$$

- (5) Mutual information update for variable nodes.

$$I_{Av}(i, j) = I_{Ec}(i, j). \quad (20)$$

- (6) Mutual information evaluation for a posteriori probability.

$$I_{APP}(j) = J(\sqrt{\sigma_{APP}}) \quad (21)$$

3.Stop criterion.

$$I_{APP}(j) = 1, \quad \forall j = 0, 1 \dots, N-1 \quad (22)$$

The message propagation between the variable nodes and the check nodes will stop when  $I_{APP}$  converges to 1. In this algorithm,  $\sigma_{Ev}$ ,  $\sigma_{Ec}$  and  $\sigma_{APP}$  can refer to [30], [32].

Note that the proposed MI-PEXIT algorithm will converge, if the transmission distance between the two coils is lower than the threshold  $d^*$ . The threshold is the highest value when the above algorithm is satisfied with the stop criterion, and it is the maximum distance that the signal can be transmitted successfully for a certain QC-LDPC code in MI communication system.

D. PROPOSED DPMIP ALGORITHM

In this section, we propose a novel optimized method for QC-LDPC code of MI communication system, which combine the discrete PSO algorithm with the MI-PEXIT algorithm. Consider the size of the parity check matrix  $\mathbf{H}$  is  $ML \times NL$ .  $L$  is the size of its sub-matrix and  $M \times N$  is the size of its base matrix  $B(H)$ .

As described in (8), the parity check matrix  $\mathbf{H}$  is composed of the information portion  $H_I$  and the parity portion  $H_P$  [26]. The base matrix of  $H_P$  is assumed to be determined for implementing the low complexity encoder. Thus the base matrix of  $H_I$ ,  $B(H_I)$  is to be optimized.

Furthermore, in the proposed DPMIP algorithm, the ‘‘particle’’ is the vector based on  $B(H_I)$ , and the ‘‘fitness value’’ of each ‘‘particle’’ is the distance threshold calculated by the MI-PEXIT method.

The details are described as follows.

1.Initialization.

Firstly, the maximum iteration numbers  $I_{max}$  and the number of ‘‘particles’’  $P_{num}$  are given. Then, the iteration number  $i = 1$ , and the  $pbest^{i=1}$  is set to be a small value.

2.Optimized vector generation.

We randomly generate  $P_{num}$  binary vectors  $\vec{W}_b$ . The optimized binary vector  $\vec{W}_b$  corresponds to the base matrix  $B(H_I)$ , and  $L_{W_b}$  is the length of  $\vec{W}_b$ .  $w_{b,pj}$  is the  $j$ -th bit of  $\vec{W}_b$  of the  $p$ -th particle,  $w_{b,pj} \in \{0, 1\}$ ,  $0 \leq j \leq L_{W_b} - 1$ .

Then,  $P_{num}$  matrices are constructed for evaluation in the next step.

3.Threshold evaluation of the ‘‘particles’’.

In this step, we evaluate the distance threshold of the QC-LDPC code by MI-PEXIT algorithm. Firstly,  $\vec{W}_b$  is converted to the base matrix  $B(H_I)$ . Then, we combine  $B(H_I)$  and  $B(H_P)$  to construct the base matrix of QC-LDPC code,  $B(H)$ .

For  $P_{num}$  binary vectors generated in step 2, we can obtain  $P_{num}$  distance thresholds  $p_{best}^i$ . Then, we can get the global ‘‘best’’ value  $g_{best}^i$  by comparing all the  $P_{num}$  thresholds  $p_{best}^i$ .

4.The binary vectors update.

Firstly, the velocity of the particle is updated as follows.

$$v_{pj}^i = \lambda v_{pj}^{i-1} + \delta(pb_{best}) + \delta(g_{best}), \tag{23}$$

where  $\lambda = 1.0$ , and  $\delta(pb_{best})$  and  $\delta(g_{best})$  are described as the following equations.

$$\delta(pb_{best}) = c_1 \eta_1 (pb_{best}_{pj}^{i-1} - w_{b,pj}^{i-1}) \tag{24}$$

$$\delta(g_{best}) = c_2 \eta_2 (g_{best}_{ij}^{i-1} - w_{b,pj}^{i-1}) \tag{25}$$

where  $c_1 = c_2 = 2.0$ , and the coefficients  $\eta_1$  and  $\eta_2$  are random numbers with the uniform distribution in (0,1) [35]. Then, the binary vector can be updated as follows.

$$w_{b,pj}^i = \begin{cases} 1, & r_{pj}^i < sig(v_{pj}^i) \\ 0, & r_{pj}^i \geq sig(v_{pj}^i), \end{cases} \tag{26}$$

where  $w_{b,pj}$  is the  $j$ -th bit of the  $p$ -th particle  $\vec{W}_b$ , and  $r_{pj}^i$  is a random number with a uniform distribution in (0,1).

Note that  $sig(v_{pj}^i)$  is described by the follows [35], [41].

$$sig(v_{pj}^i) = \frac{1}{1 + e^{-v_{pj}^i}}, \tag{27}$$

5.Stop criterion.

Furthermore, we update the iteration number  $i = i + 1$ . Then, go to step (3), evaluate the new vectors. Consequently the  $pb_{best}$  and  $g_{best}$  is updated until  $I_{max}$  is achieved.

Finally, we obtain the optimized base matrix, which corresponds to the best distance threshold.

V. SIMULATION RESULTS AND ANALYSIS

In this section, we firstly investigate the path loss of MI channel with different coil radii. Then, two groups of QC-LDPC codes are constructed by the proposed DPMIP algorithm in the simulation, which are named as code A and code B. In the simulation, the number of the ‘‘particles’’  $P_{num} = 20$ , and the maximum iteration numbers  $I_{max} = 30$ .

The size of the sub-matrix  $L$  of the proposed codes is set to be 96 for fair comparison with the QC-LDPC codes in 802.16e standard (802.16e code) [23]. Note that the base matrix of the 802.16e code is composed of two parts, which

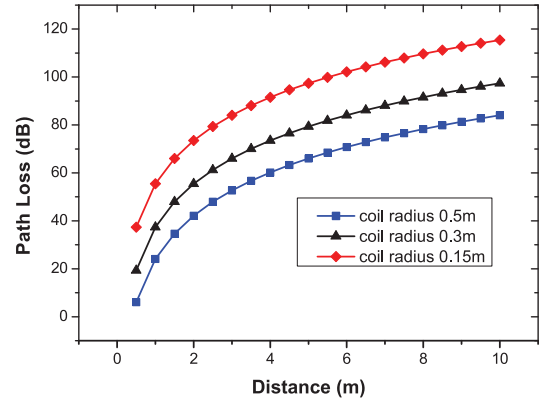


FIGURE 5. Path loss comparison for different coil radius.

TABLE 1. Code parameters of the proposed code A.

Name	Code rate	Optimized vector size	Base matrix size	Code length
code A1	1/2	144	12 × 24	2304
code A2	1/3	72	12 × 18	1728
code A3	1/4	48	12 × 16	1536

correspond to the systematic bits and the parity check bits, respectively. There are six base matrices and the corresponding exponent matrices are given in [23].

The path loss comparison for different coil radii is described as Fig.5. The path loss of MI channel is given as equation (3). The other parameters is the same as in [1] besides the coil radius.

From Fig.5, we can see that when the distance is 2m, the path loss of the coils with coil radius 0.15m, 0.3m and 0.5m are about 73dB, 55dB and 42dB, respectively. The largest coil radius results in about 31dB gain. On the other side, when the path loss is about 55dB, the distance with coil radius 0.15m, 0.3m and 0.5m are about 1m, 2m and 3.5m, respectively. The largest coil radius achieves about 2.5m improvement for the same path loss.

Thus, in this study, we take the coil radius into account when constructing the QC-LDPC codes for MI communication system.

A. DISTANCE THRESHOLDS OF THE PROPOSED CODES

For code A, we construct three QC-LDPC codes, which are optimized with the same coil parameters. The coil parameters are the same as in [1], the transmission power  $P_t = 10dBm$ , the noise power  $P_n = -103dBm$ , the radii of the transmitter and receiver coil  $a_t, a_r$  are both 0.15m, and the number of turns of the transmitter and receiver coil are both 5. The code parameters of code A are given as follows.

The distance thresholds of code A1, code A2 and code A3 are obtained by the proposed DPMIP algorithm, which are given in table 2.

Note that to keep the low encoding complexity of QC-LDPC codes, we have to keep the  $H_P$  unchanged. Thus we punctured some columns of  $H_I$  of code A1 to construct the QC-LDPC codes with code rate 1/3 and 1/4. Lower code

**TABLE 2. Distance thresholds of the proposed code A.**

code A1	code A2	code A3
$8.4m$	$8.42m$	$8.37m$

**TABLE 3. Coil parameters of the proposed code B.**

Name	transmission power(dBm)	noise power(dBm)	coil radius(m) $a_t, a_r$	coil turn $N_t, N_r$
code B1	10	-103	0.3, 0.3	5,5
code B2	30	-103	0.15,0.15	5,5
code B3	30	-103	0.3,0.3	5,5

**TABLE 4. Distance thresholds of the proposed code B.**

code B1	code B2	code B3
$17.16m$	$18.48m$	$36.91m$

rate usually leads to better distance threshold, and however shorter code length usually results in smaller distance threshold. From the obtained thresholds, we can see that code A2 achieve a good trade-off between the code rate and the code length, which has the best distance threshold.

Therefore, for code B, another three QC-LDPC codes are constructed with different coil radii or different transmission power, which all have the same code parameters as that of code A2. To simplify the description, the three QC-LDPC codes are regarded as different coil parameters. Performance comparison among code B may better reveal the effect of the coil parameters on the code performance for MI communication system.

The coil parameters of these codes are described in table 3.

Note that for fair comparison and easy simulation, the three codes of code B have the same noise power and the turn of coil. The noise power is the average power, and the turn is the typical value [1].

The optimal three matrices of the code B are constructed by the DPMIP algorithm, and meanwhile their corresponding distance threshold are obtained, which are described in table 4.

We can combine the optimal matrix  $H_I$  with  $H_P$  which is given as (9), and construct the corresponding three  $H$  matrices.

Note that we predict the best distance threshold with the determined coil parameters of code B by the proposed DPMIP algorithm, which lead to an easy way for evaluating and designing MI communication system based on QC-LDPC codes.

**B. BASE MATRIX AND H MATRIX OF PROPOSED CODES**

The three optimal base matrices of code A1, code A2 and code A3 are given in Fig.6.

From Fig.6 we can see that the cross represents “1” in the base matrix which corresponds to the nonzero submatrix in  $H$  matrix, and while the blank area represents the zero which corresponds to the zero sub-matrix in  $H$ . Note that the three matrices share the same last 12 columns, which corresponds to the  $B(H_P)$ .

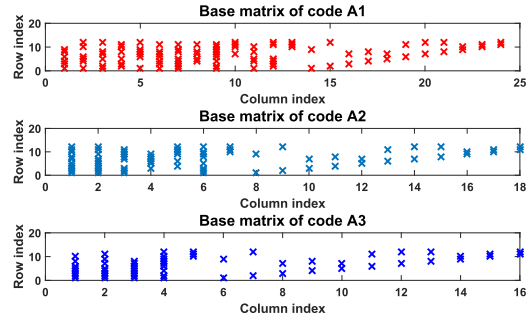


**FIGURE 6. Base matrix of code A.**

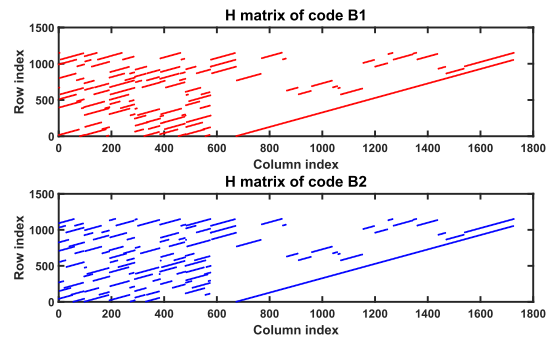


**FIGURE 7. H matrix of code B1 and code B2.**

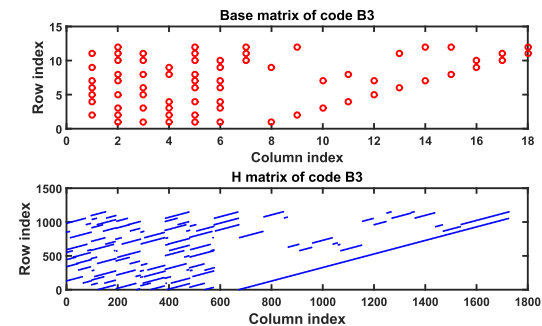


**FIGURE 8. Base matrix and H matrix of code B3.**

The parity check matrices of code B1 and code B2 are described in Fig.7. The base matrix and the corresponding parity check matrix of code B3 are given in Fig.8. As shown in table 3, the three QC-LDPC codes of code B have the same code rate and code length as that of code A2. Thus, we investigate the effect of the coil radius and the transmitting power of code B.

From Fig.7 and Fig.8, we can see that the  $H$  matrices of code B1, code B2 and code B3 have the same portion, which is from column 577 to column 1728 (the last column). During the optimization, we only search the optimal base matrix  $B(H_I)$ , and the  $B(H_P)$  has to be unchanged to guarantee the simple recursive form of encoding QC-LDPC codes.

The optimal base matrix of the QC-LDPC codes will be obtained when we combine the  $B(H_I)$  with the  $B(H_P)$ , and then we can construct the  $H$  matrix of the QC-LDPC codes. Note that for simplifying the simulation, the non-zero entries of the exponent matrices are randomly generated



in  $[0, L - 1]$ , and simulation results shows that this simplification is reasonable.

**C. DISTANCE THRESHOLD EVOLUTION AND MUTUAL INFORMATION EVOLUTION**

The distance threshold is an important parameter to evaluate the performance of QC-LDPC codes for MI communication system. For each discrete (binary) PSO iteration, the predetermined numbers of matrices are evaluated by the MI-PEXIT algorithm, and the best distance threshold will be found when the maximum iteration numbers  $I_{max}$  is achieved. During the evaluation for each matrix, the mutual information will decrease if the distance increases.

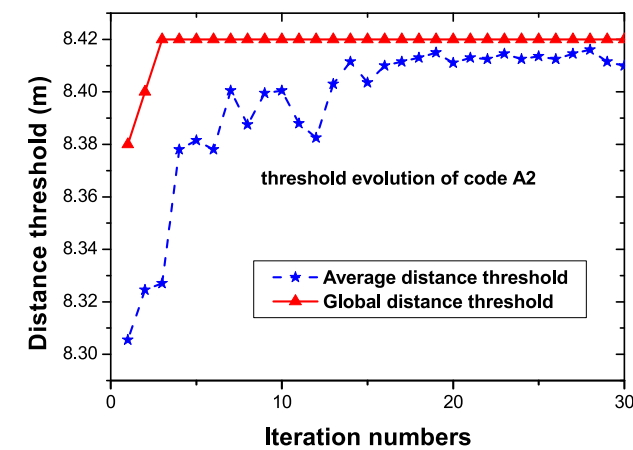


FIGURE 9. Distance threshold evolution of code A2.

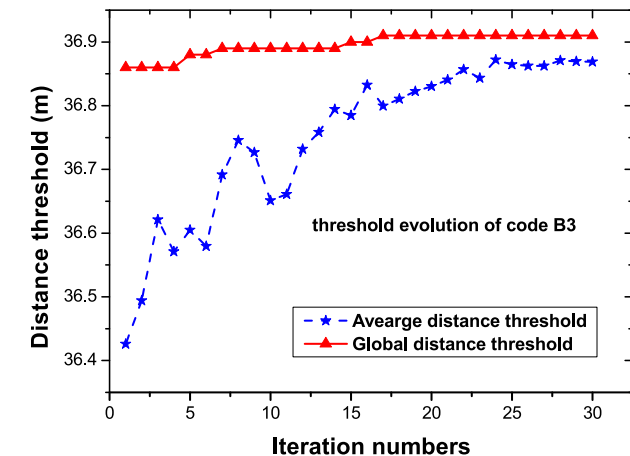


FIGURE 10. Distance threshold evolution of code B3.

The distance threshold evolution of code A2 and code B3 are given in Fig.9 and Fig.10. In these two figures, the average distance threshold evolution and the global distance threshold evolution are given respectively.

From Fig.9 and Fig.10, we can see that the distance thresholds of code A2 and code B3 are  $8.42m$  and  $36.91m$ , which is given in table 2 and table 4. For code A2, the distance threshold  $8.42m$  is obtained when the iteration number is 3,

and while for code B3, the distance threshold  $36.91m$  is achieved when the iteration number is 17.

To further reveal the relation between the mutual information and the distance during the optimization, the mutual information evolution of code B1, code B2 and code B3 are given in Fig.11. In this figure, the mutual information of each code decrease from 1 sharply when the distance increase above their distance thresholds respectively, which verify the “distance threshold effect” of QC-LDPC codes of the MI communication system. Note that the mutual information of the QC-LDPC codes is “1” means successfully decoding the message.

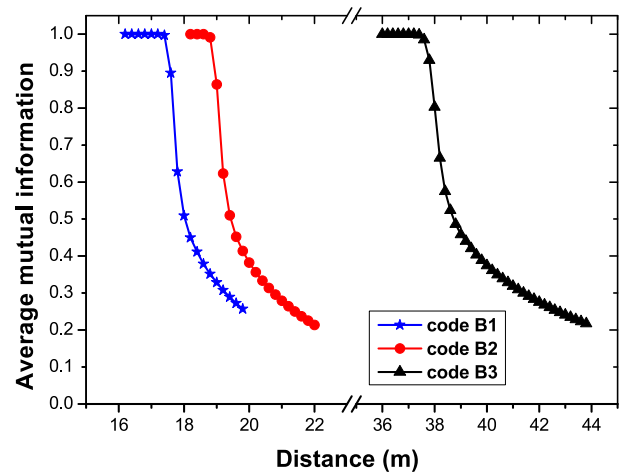


FIGURE 11. Mutual information evolution for code B.

**D. BER COMPARISON**

To better validate the superiority of our proposed code in WUSN, we also compare the performance of 802.16e code and the proposed code A1. In this study, the code parameters of 802.16e code is the same as that of code A1, which has the code rate 1/2 and the code length 2304. Note that 802.16e code is originally designed for EM wave communication [23].

Firstly, we use the 802.16e code in MI communication system, and compare the BER of coded simulation and the uncoded simulation. Then, to verify the better performance of our proposed code, we compare the BER between code A1 and 802.16e code.

BER comparison for MI communication between coded and uncoded simulation is described as Fig.12. In this figure, the BER of uncoded theoretical result is calculated from  $BER = 0.5 * erfc(\sqrt{SNR})$  [1]. The coded simulation is performed by using the 802.16e code in MI communication system described in Fig.3. From this figure, we can see that the coded simulation perform much better than the uncoded result in terms of BER.

Furthermore, the BER comparison of code A1 and 802.16e code is given in Fig.13. From this figure, code A1 achieve about  $4.4m$  improvement than the 802.16e code at BER of  $10^{-4}$ . Thus, the proposed codes achieve a better

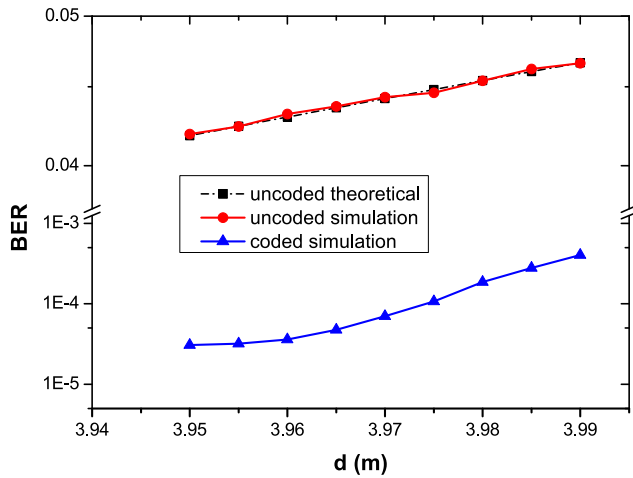


FIGURE 12. BER comparison for MI communication between uncoded and coded simulation.

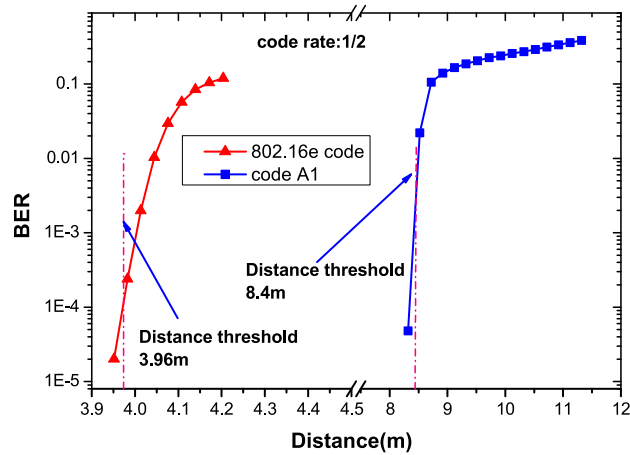


FIGURE 13. BER comparison for code A1 and 802.16e code.

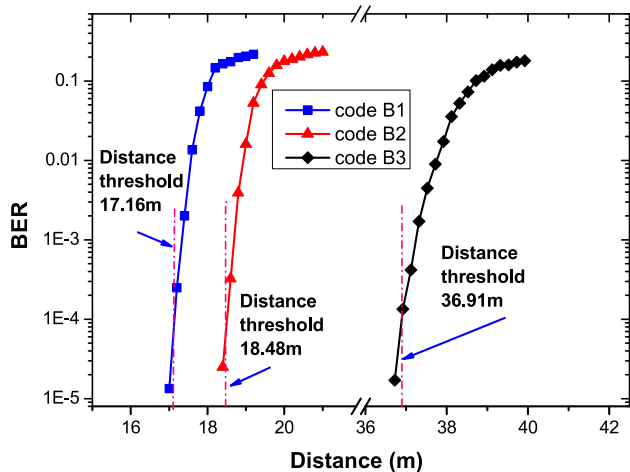


FIGURE 14. BER comparison for code B.

performance than 802.16e code, which verify the superiority of the proposed DPMIP algorithm.

BER comparison of code B is given in Fig.14. From this figure, we can see that the distances of BER at  $10^{-4}$  of

code B1, code B2 and code B3 are in good agreement with their distance thresholds, respectively. Therefore, it can be deduced that the proposed DPMIP algorithm can predict the distance threshold well while optimizing the QC-LDPC codes for MI communication system.

## VI. CONCLUSION

In this study, we propose a novel scheme, DPMIP algorithm, to optimize the QC-LDPC codes for MI-based WUSN, which combine the PSO method with the proposed MI-PXIT algorithm. We can predict the distance threshold of the optimized QC-LDPC codes by the proposed scheme besides constructing the optimal QC-LDPC codes for MI communication system.

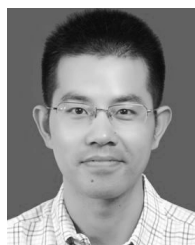
Simulation results show that the proposed scheme is a desirable method to design the QC-LDPC codes for MI-based WUSN. It provides an easy method to evaluate the performance of MI communication system based on QC-LDPC codes, and it also provide a guideline to design the parameters of MI communication system such as the coil radius, transmitting power.

Note that we only consider the direct magnetic communication in this study. Channel model is the difference between the direct MI and the MI waveguides [28]. Thus the proposed method can also be extended to construct QC-LDPC codes for MI waveguides.

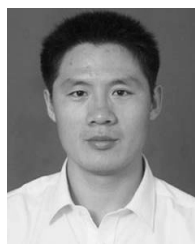
## REFERENCES

- [1] Z. Sun and I. F. Akyildiz, "Magnetic induction communications for wireless underground sensor networks," *IEEE Trans. Antennas Propag.*, vol. 58, no. 7, pp. 2426–2435, Jul. 2010.
- [2] T. E. Abrudan, O. Kypris, N. Trigoni, and A. Markham, "Impact of rocks and minerals on underground magneto-inductive communication and localization," *IEEE Access*, vol. 4, pp. 3999–4010, 2016.
- [3] Z. Sun and I. F. Akyildiz, "Spatio-temporal correlation-based density optimization in wireless underground sensor networks," in *Proc. IEEE Global Telecommun. Conf. (GLOBECOM)*, Dec. 2011, pp. 1–5.
- [4] Z. Sun and I. F. Akyildiz, "On capacity of magnetic induction-based wireless underground sensor networks," in *Proc. IEEE INFOCOM*, Mar. 2012, pp. 370–378.
- [5] S. Kisseleff, W. Gerstacker, Z. Sun, and I. F. Akyildiz, "On the throughput of wireless underground sensor networks using magneto-inductive waveguides," in *Proc. IEEE Global Telecommun. Conf. (GLOBECOM)*, Dec. 2013, pp. 322–328.
- [6] S. Kisseleff, I. F. Akyildiz, and W. H. Gerstacker, "Digital signal transmission in magnetic induction based wireless underground sensor networks," *IEEE Trans. Commun.*, vol. 63, no. 6, pp. 2300–2311, Jun. 2015.
- [7] X. Tan, Z. Sun, and I. F. Akyildiz, "Wireless underground sensor networks: MI-based communication systems for underground applications," *IEEE Antennas Propag. Mag.*, vol. 57, no. 4, pp. 74–87, Aug. 2015.
- [8] H. Guo, Z. Sun, and P. Wang, "Channel modeling of MI underwater communication using tri-directional coil antenna," in *Proc. IEEE Global Commun. Conf. (GLOBECOM)*, Dec. 2015, pp. 1–6.
- [9] I. F. Akyildiz, P. Wang, and Z. Sun, "Realizing underwater communication through magnetic induction," *IEEE Commun. Mag.*, vol. 53, no. 11, pp. 42–48, Nov. 2015.
- [10] X. Tan and Z. Sun, "On environment-aware channel estimation for wireless sensor networks using magnetic induction," in *Proc. IEEE Conf. Comput. Commun. Workshops (INFOCOM WKSHPS)*, May 2017, pp. 217–222.
- [11] Z. Li and Z. Sun, "Antenna system optimization for active metamaterial-enhanced magnetic induction communications," in *Proc. 13th Eur. Conf. Antennas Propag. (EuCAP)*, 2019, pp. 1–5.

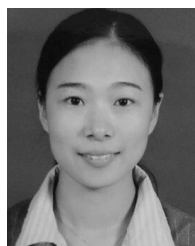
- [12] S. Kisseleff, I. F. Akyildiz, and W. H. Gerstacker, "Magnetic induction-based simultaneous wireless information and power transfer for single information and multiple power receivers," *IEEE Trans. Commun.*, vol. 65, no. 3, pp. 1396–1410, Mar. 2017.
- [13] H. Saeedi and A. Banihashemi, "Systematic design of low-density parity-check code ensembles for binary erasure channels," *IEEE Trans. Commun.*, vol. 58, no. 1, pp. 118–127, Jan. 2010.
- [14] H. Saeedi and A. H. Banihashemi, "On the design of LDPC code ensembles for BIAWGN channels," *IEEE Trans. Commun.*, vol. 58, no. 5, pp. 1376–1382, May 2010.
- [15] J. Hou, P. H. Siegel, and L. B. Milstein, "Performance analysis and code optimization of low density parity-check codes on Rayleigh fading channels," *IEEE J. Sel. Areas Commun.*, vol. 19, no. 5, pp. 924–934, May 2001.
- [16] H. Xu, "Bilayer lengthened QC-LDPC codes design for relay channel," *IEICE Trans. Commun.*, vol. 97, no. 7, pp. 1365–1374, 2014.
- [17] H. Xu, "Construction of quasi-cyclic low-density parity-check codes with low encoding complexity," *Int. J. Commun. Syst.*, vol. 27, no. 8, pp. 1201–1216, 2014.
- [18] D. Chen, N. Zhang, R. Lu, X. Fang, K. Zhang, Z. Qin, and X. Shen, "An LDPC code based physical layer message authentication scheme with perfect security," *IEEE J. Sel. Areas Commun.*, vol. 36, no. 4, pp. 748–761, Apr. 2018.
- [19] X. Dong and M. C. Vuran, "Exploiting soil moisture information for adaptive error control in wireless underground sensor networks," in *Proc. IEEE Global Commun. Conf.*, Dec. 2013, pp. 97–102.
- [20] R. M. Tanner, D. Sridhara, A. Sridharan, T. E. Fuja, and D. J. Costello, Jr., "LDPC block and convolutional codes based on circulant matrices," *IEEE Trans. Inf. Theory*, vol. 50, no. 12, pp. 2966–2984, Dec. 2004.
- [21] M. P. C. Fossorier, "Quasi cyclic low-density parity-check codes from circulant permutation matrices," *IEEE Trans. Inf. Theory*, vol. 50, no. 8, pp. 1788–1793, Aug. 2004.
- [22] L. Lan, L. Zeng, Y. Y. Tai, L. Chen, S. Lin, and K. Abdel-Ghaffar, "Construction of quasi-cyclic LDPC codes for AWGN and binary erasure channels: A finite field approach," *IEEE Trans. Inf. Theory*, vol. 53, no. 7, pp. 2429–2458, Jul. 2007.
- [23] *IEEE Standard for local metropolitan area networks. Part 16: Air Interface for Fixed and Mobile Broadband Wireless Access Systems, Amendment 2*, IEEE Standard 802.16e-2005, Feb. 2006.
- [24] J. Perez and V. Fernandez, "Low-cost encoding of IEEE 802.11 n," *Electron. Lett.*, vol. 44, no. 4, pp. 307–308, 2008.
- [25] Z. Cai, J. Hao, P. Tan, S. Sun, and P. Chin, "Efficient encoding of IEEE 802.11n LDPC codes," *Electron. Lett.*, vol. 42, no. 25, pp. 1471–1472, Dec. 2006.
- [26] W. Tam, F. Lau, and C. Tse, "A class of QC-LDPC codes with low encoding complexity and good error performance," *IEEE Commun. Lett.*, vol. 14, no. 2, pp. 169–171, 2010.
- [27] S. Kisseleff, I. F. Akyildiz, and W. H. Gerstacker, "Throughput of the magnetic induction based wireless underground sensor networks: Key optimization techniques," *IEEE Trans. Commun.*, vol. 62, no. 12, pp. 4426–4439, Dec. 2014.
- [28] S. C. Lin, I. F. Akyildiz, P. Wang, and Z. Sun, "Distributed cross-layer protocol design for magnetic induction communication in wireless underground sensor networks," *IEEE Trans. Wireless Commun.*, vol. 14, no. 7, pp. 4006–4019, Jul. 2015.
- [29] T. J. Richardson and R. L. Urbanke, "The capacity of low-density parity-check codes under message-passing decoding," *IEEE Trans. Inf. Theory*, vol. 47, no. 2, pp. 599–618, Feb. 2001.
- [30] G. Liva and M. Chiani, "Protograph LDPC codes design based on EXIT analysis," in *Proc. IEEE Global Telecommun. Conf. (GLOBECOM)*, Nov. 2007, pp. 3250–3254.
- [31] J. Thorpe, "Low-density parity-check (LDPC) codes constructed from protographs," JPL, IPN Progr., Pasadena, CA, USA, Tech. Rep. 42-154, 2005.
- [32] X. Liu, X. Wu, and C. Zhao, "Shortening for irregular QC-LDPC codes," *IEEE Commun. Lett.*, vol. 13, no. 8, pp. 612–614, Aug. 2009.
- [33] S. Myung and K. Yang, "A combining method of quasi-cyclic LDPC codes by the Chinese remainder theorem," *IEEE Commun. Lett.*, vol. 9, no. 9, pp. 823–825, Sep. 2005.
- [34] J. Kennedy and R. Eberhart, "Particle swarm optimization," in *Proc. IEEE ICNN*, vol. 4, Nov./Dec. 1995, pp. 1942–1948.
- [35] N. Jin and Y. Rahmat-Samii, "Advances in particle swarm optimization for antenna designs: Real-number, binary, single-objective and multiobjective implementations," *IEEE Trans. Antennas Propag.*, vol. 55, no. 3, pp. 556–567, Mar. 2007.
- [36] C. N. Ko, Y. P. Chang, and C. J. Wu, "A PSO method with nonlinear time-varying evolution for optimal design of harmonic filters," *IEEE Trans. Power Syst.*, vol. 24, no. 1, pp. 437–444, Feb. 2009.
- [37] I. Kamrul and E. Oki, "PSO: Preventive start-time optimization of OSPF link weights to counter network failure," *IEEE Commun. Lett.*, vol. 14, no. 6, pp. 581–583, Jun. 2010.
- [38] L. Lizzi, F. Viani, R. Azaro, and A. Massa, "Optimization of a spline-shaped UWB antenna by PSO," *IEEE Antennas Wireless Propag. Lett.*, vol. 6, pp. 182–185, 2007.
- [39] T. Wimalajeewa and S. K. Jayaweera, "Optimal power scheduling for correlated data fusion in wireless sensor networks via constrained PSO," *IEEE Trans. Wireless Commun.*, vol. 7, no. 9, pp. 3608–3618, Sep. 2008.
- [40] S. ten Brink, G. Kramer, and A. Ashikhmin, "Design of low-density parity-check codes for modulation and detection," *IEEE Trans. Commun.*, vol. 52, no. 4, pp. 670–678, Apr. 2004.
- [41] J. Kennedy and R. C. Eberhart, "A discrete binary version of the particle swarm algorithm," in *Proc. IEEE Int. Conf. Syst., Man, Cybern. Comput. Simulation*, vol. 5, Oct. 1997, pp. 4104–4108.



**HUA XU** received the M.S. degree from Soochow University, China, in 2003, and the Ph.D. degree from the Nanjing University of Posts and Telecommunications, China, in 2007. From August 2010 to February 2011, he was a Visiting Scholar with the BCWS Centre, Carleton University, Canada. He is currently a Professor with the School of Physics and Electronic Engineering, Yancheng Teachers University, China. His research interests include LDPC codes design, compressed sensing, and magnetic induction communication.



**YANJING SUN** received the Ph.D. degree in information and communication engineering from the China University of Mining and Technology, in 2008, where he is currently a Professor with the School of Information and Control Engineering, since July 2012. He is also a Vice Director of the Coal Mine Electrical Engineering and Automation Laboratory in Jiangsu Province. His current research interests include IBFD communication, embedded real-time systems, wireless sensor networks, and cyber physical systems.



**WENJUAN SHI** received the master's degree from Soochow University, China, in 2006, and the Ph.D. degree from the China University of Mining and Technology, in 2018. She is currently an Associate Professor with the School of Physics and Electronic Engineering, Yancheng Teachers University, China. Her current research interests include wireless communication and data mining.